ISSN 1028-334X, Doklady Earth Sciences, 2006, Vol. 411, No. 8, pp. 1229–1232. © Pleiades Publishing, Inc., 2006.
Original Russian Text © Yu.V. Laptev, K.B. Rozov, 2006, published in Doklady Akademii Nauk, 2006, Vol. 410, No. 5, pp. 663–667.

GEOCHEMISTRY

Interaction of Gold with Sulfide Surface As a Factor of Its Concentration in Hydrothermal Ore Formation

Yu. V. Laptev[a] and K. B. Rozov[b]

Presented by Academician N.V. Sobolev December 29, 2005

Received January 11, 2006

DOI: 10.1134/S1028334X06080150

In recent years, substantial progress has been achieved in systematization of internal relationships between different states of the implicit Au in sulfide minerals not only on the basis of up-to-date analytical methods but also from the theoretical standpoint of crystal chemistry [1–3]. It has been shown that perfection of the matrix structure of the host mineral [2] and the homogeneity of Au distribution [3] serve as criteria of the structural state of gold. The concentration of Au in extrastructure sites is considered in terms of the endocryptic concept (localization of atoms with participation of crystal lattice defects) [2, 4]. The decrease in perfection of pyrite crystals along with a decrease in their dimensions from 1.5 to 0.3 mm leads to an increase in the content of extrastructure Au from 22 to 77% [3].

The active Au concentration in extrastructure sites provides for a more complicate mechanism of its conservation than the direct joint crystallization with the formation of solid solutions [4]. It is suggested that the initial interaction of dissolved Au with the sulfide surface serves as a factor of its subsequent mobilization by the solid phase. The intensity of development of this stage depends on the possibility to form surficial complexes in the succession of interactions: solution ↔ surface ↔ crystal. Researchers have presented several pieces of evidence of Au extraction by means of adsorption at the sulfide surface for various types of ore-forming processes [5], in particular, for the Carlin-type deposits [6] and modern deposits in oceanic basins [7]. The physicochemical study of reactivity of the sulfide surface to interaction with heavy and noble metals has been performed largely making use of chloride Au(III) solutions (see, for example, [8, 9]). This substance poorly fits the redox conditions of hydrothermal processes with the predominance of dissolved Au(I) species.

The objective of this study is to investigate distribution of Au(I) between the subacid chloride–sulfide solution and the sulfide (pyrite) surface at an elevated temperature (200°C, P = 150–200 bars) as a factor that controls the possibility of the subsequent conservation of Au in implicit forms during the growth of sulfide crystals. The experimental technique was characterized by the following specific features.

(1) We used the method of competitive reactions, when the total consumption of Au introduced as excess quantities of Au(met) was determined by the intensity of its dissolution and the subsequent precipitation according to the scheme: Au(met) ↔ Au(solution) ↔ Au(≡FeS_2).

(2) The maximum Au solubility in subacid sulfide–chloride solutions was provided by intermediate values of the redox potential between pyrite–pyrrhotite and pyrite–hematite mineral buffers. The essence of this technique consists in the addition of rigorously dosed amounts of oxidant (nitric acid) to the sulfide–chloride (0.1$m$$H_2S$ + 0.17mNaCl) solution up to 0.00156m HNO_3 concentration (pH = 2.9). It was established that the dissolved species of elementary sulfur S_8^0(solution) is a product of hydrogen sulfide oxidation at the level of $n \cdot 10^{-4}m$ (or a fraction of a percent of m_{H_2S}). The $m_{H_2(solution)}$ concentrations were calculated through experimentally determined m_{H_2S} and $m_{S_8^0(solution)}$ based on the equilibrium constant

$$8H_2(solution) + S_8(solution) \leftrightarrow 8H_2S(solution). \quad (1)$$

The experiments were carried out in titanium autoclaves with a fluoroplastic insert at t = 200°C and P = 150–200 bars. Pyrite was synthesized with the hydrothermal method under gradient conditions (t = 420–400°C, P = 500 bars). The phase homogeneity of pyrite (ground to a grain size of <30–60 μm) was controlled

[a] *Institute of Geology and Mineralogy, Siberian Division, Russian Academy of Sciences, pr. akademika Koptyuga 3, Novosibirsk, 630090 Russia; e-mail: laptev@uiggm.nsc.ru*

[b] *Novosibirsk State University, ul. Pirogova 2, Novosibirsk, 630090 Russia*

Table 1. Composition of solutions after the runs on dissolution of Au (V = 38 ml) at T = 200°C and P = 200 bars at different durations

Run	τ, h	m_{H_2S}, ±0.01	$m_{S_8^0}$, $n \cdot 10^{-4}$	pH_{meas}, ±0.05	Loss of Au mass, ±5 μg	m_{Au}, $n \cdot 10^{-5}$	
						based on loss of mass	based on chemical analysis
48-2	3.15	0.12	1.0 ± 0.1	2.90	13	0.17 ± 0.07	0.23 ± 0.02
48-1	4.0	0.12	0.9 ± 0.09	3.30	23	0.31 ± 0.07	0.41 ± 0.04
49-1	9.2	0.12	–	4.70	43	0.57 ± 0.07	–
50-1	15.0	0.11	1.0 ± 0.1	4.88	79	1.06 ± 0.07	1.35 ± 0.13
45-2	21.0	0.12	–	4.87	221	2.95 ± 0.07	2.73 ± 0.20
51-1	24.0	0.11	2.2 ± 0.2	4.96	286	3.82 ± 0.07	3.53 ± 0.20
47-1	26.0	0.11	–	5.00	275	3.67 ± 0.07	3.51 ± 0.20
49-2	30.0	0.12	–	5.10	287	3.83 ± 0.07	–

by optical microscopy, X-ray methods, and scanning electron microscopy. To provide an equally accessible surface, the autoclave was rotated around a transverse axis in the course of runs (duration up to 30 h).

Table 1 presents the results of experiments (from 3.15 to 30 h long) on Au dissolution. The data obtained are virtually completely (within ±10%) consistent with the results based on the method of loss of the gold foil mass and the chemical analysis of liquid samples. The time of achievement of the steady compositional state of the solution was 24 h.

We calculated a model solubility of Au under run conditions on the basis of minimization of free energy using the HCh software package [10] and the UNITHERM thermodynamic data set. The parameters of the HKF equation for G^0 value of dissolved $Au(HS)^0$ and $Au(HS)_2^-$ species were taken from [11]. The G^0 values for S_8^0(solution) after [12] were adapted to the HKF equation by empirical fitting of its coefficients. As was expected [11], the prevalent species of the dissolved Au is represented by $Au(HS)^0$, which accounts for 66% of the total concentration of $Au(HS)^0$ and $Au(HS)_2^-$. The calculated solubility of Au turned out to be lower than the experimentally determined value by 16% ($3.2 \cdot 10^{-5}m$ versus $3.7 \pm 0.2 \cdot 10^{-5}m$), and this difference exceeds experimental errors (Table 1).

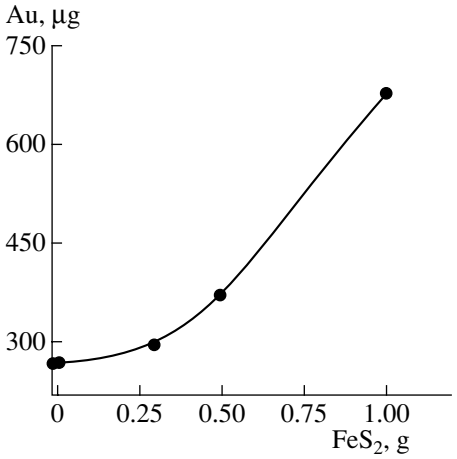

Fig. 1. Relationship between the total Au consumption and the amount of FeS_2 under run conditions.

The distinct effect of the increase in the total Au consumption depending on the amount of FeS_2 is observed in experiments with pyrite (Fig. 1). The Au balance by the sum of its chemical analytical determinations in solution and pyrite is fulfilled within 10% relative to the loss of the gold foil mass. The total Au consumption versus the pyrite charge linear relationship is disturbed due to the different degrees of solid phase grinding. The SEM study of pyrite (Fig. 2) did not reveal individual Au-bearing phases. Table 2 shows the results of calculation of the apparent partition coefficient K_D, i.e., the ratio of the Au concentration in the solid phase ($Au_{\equiv FeS_2, ppm}$, ppm) to its concentration in solution ($Au_{solution, ppm}$, ppm). Although the effect of redistribution of Au between solution and pyrite has been established, more precise determination of the partition coefficient requires additional experimental study.

In order to determine speciation of Au precipitates from acid sulfide solutions, the runs were performed according to a simplified scheme: Au(solution) → Au(precipitate). The 1-h-long experiment was conducted by introducing dosed amounts of HCl into the Au-bearing ($0.12m H_2S + 0.1m NaOH + 1.2 \cdot 10^{-3}m Au$) solution up to pH = 2.5 through a lock screw at T = 200°C. In the absence of pyrite, the product of precipitation was a phase, the X-ray pattern of which indicates a cubic structure with a = 5.02 that corresponds to both Au_2S [13] and high-temperature modification of AgAuS (JCPDS 26-0728).

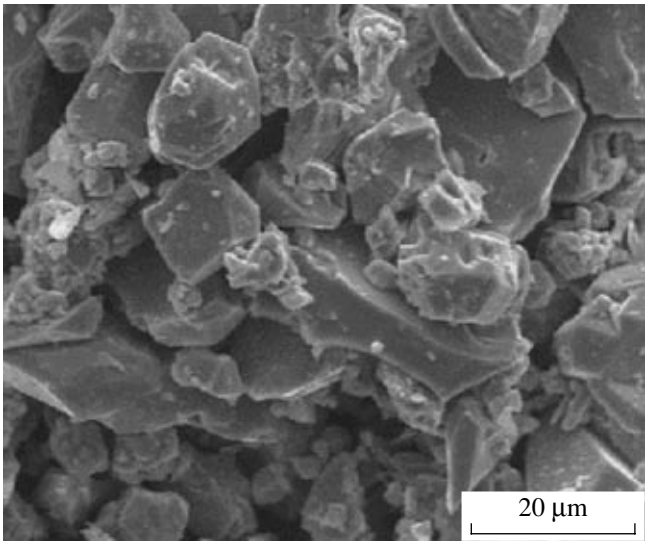

Fig. 2. SEM photomicrograph of pyrite from the run on Au precipitation.

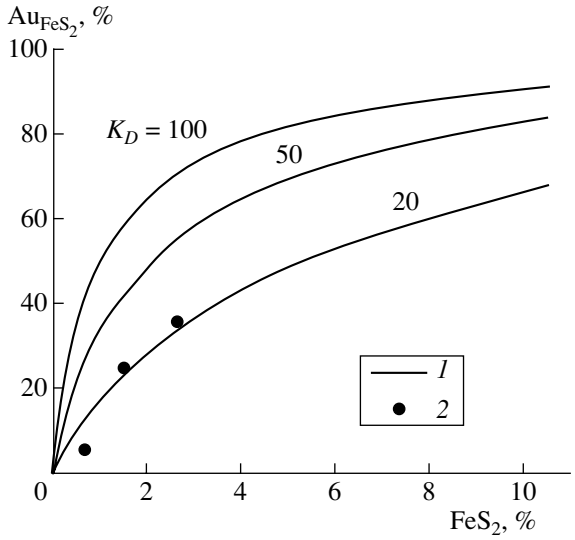

Fig. 3. Percentage of "pyritic" Au vs. mass ratio FeS_2/solution at different apparent partition coefficients K_D (calculated forecast in comparison with experimental data). (*1*) Calculation, (*2*) experiment.

The precipitation of gold using the same technique but in the presence of fine-crystalline pyrite (fraction <1–2 μm, charge 0.5 g, 40 ml of solution) proceeded without formation of individual Au-bearing phases, whereas the Au content in pyrite was 3000 ppm. The method of photoelectron spectroscopy (XPS) equipped with a VG Microtech Ltd device was used to study the state of gold in this sample. The Au band $4f_{7/2}$ recorded in spectrums with a maximum of 85.1 eV differs from the band of metallic Au and its clusters (83.9–84.7 eV), but fits the surficial Au compounds in the nonmetallic state Au(I) at 84.8–85.1 eV [5]. Taking into consideration our data (see above) on the possible precipitation of gold as Au_2S, the revealed state of gold at the pyrite surface may also fit its sulfide species. This suggestion does not contradict the results obtained for Au sorption on iron sulfides (pyrrhotite and pyrite), in which a nonmetallic species "similar to Au_2S in its structural framework" was detected by the Mössbauer method [9].

The geochemical implications of the surficial interaction of Au with pyrite were estimated on the basis of Au partition coefficients obtained in experiments (Table 2) and their arbitrarily chosen values (K_D = 20, 50, 100). At the given K_D, the percentage of the precipitated Au in the material balance of the FeS_2–solution system is a function of their mass ratio (Fig. 3). The Au distribution in the experiments is close to the calculated curve at K_D = 20, and the amount of precipitated Au does not exceed 40%. If we extrapolate this curve over greater amounts of pyrite (up to 10% FeS_2 of solution mass), the percentage of the precipitated Au increases to 60–70%. At higher K_D values (50 and 100) that are possible for processes on the oceanic floor with participation of porous sulfide-bearing aggregates [7], the role of surficial interaction (SI) should be much more important even in the presence of a minor amount of solid phase (high solution/solid ratio). In the case of sulfide vein formation with the growth of large (a few millimeters across) crystals, the SI of Au may be substantial due to the low solution/solid ratio.

If the effect of surficial interaction of Au between solution and the solid phase is developed, the Au solubility as a limit of migration ability allows us to forecast the probability of realization of this mechanism in different geochemical situations. Figure 4 shows the calculated isotherm (T = 200°C and P = 150 bars) of Au solubility depending on the concentration of the dissolved hydrogen as a parameter of the redox potential. In this figure, the point of experimentally determined Au solubility is tied to m_{H_2}(solution) calculated through the equilibrium constant (1) from the experimental data on the S_8^0(solution) and H_2S(solution) concentrations. The points on the curve of Au solubility for buffer pyrite-bearing assemblages were determined by calculating m_{H_2}(solution) for equilibrium

Table 2. Initial data and results of calculation of the apparent partition coefficient (K_D) of Au between pyrite and solution based on $Au_{\equiv FeS_2} \leftrightarrow Au_{sol}$ equilibrium

FeS_2, g	Solution/solid ratio	$Au_{\equiv FeS_2}$, ppm	$Au_{p\text{-}p}$, ppm	K_D
0.3	126	35	7.2	4.8 ± 5
0.5	76	162	6.25	26 ± 5
1.0	38	257	11.5	22 ± 5

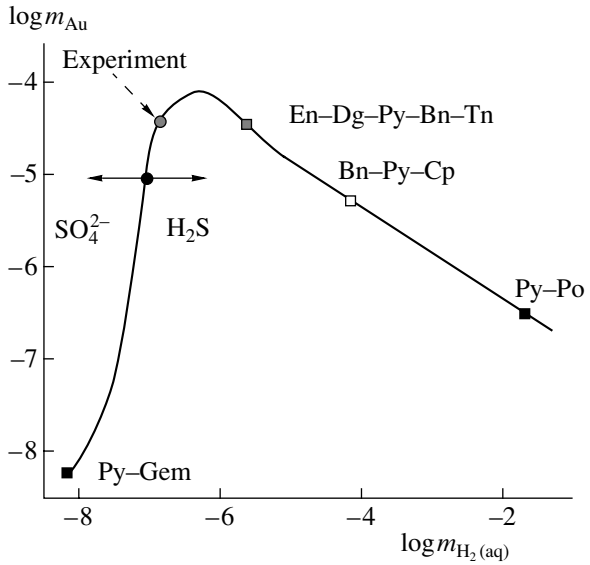

Fig. 4. Calculated Au solubility in the $0.1m H_2S$ + $0.17m$NaCl, pH 3.8 solution (pH 3.8 at T = 200°C and P = 150 bars) vs. equilibrium H_2(aq) concentrations. Points corresponding to Au solubility in the presence of buffer mineral assemblage: (Py–Hem) pyrite–hematite; (En–Dg–Py–Bn–Tn) enargite–digenite–pyrite–bornite–tennantite; (Bn–Py–Cp) bornite–pyrite–chalcopyrite; (Py–Po) pyrite–pyrrhotite. (Experiment) Point corresponding to run conditions. Arrows separate regions with a prevalence of sulfate and sulfide sulfur.

$$0.5S_2(\text{gas}) + H_2(\text{solution}) \leftrightarrow H_2S(\text{solution}) \qquad (2)$$

at the sulfur fugacity taken from [14].

The calculated and experimental values of Au solubility are closest for the enargite–digenite–pyrite–tennantite–bornite buffer (Fig. 4). Precipitation of native gold in the presence of this buffer requires a very high Au concentration in solution ($\log m_{Au}$ = –4.3 or 10 ppm). However, the effect of Au fractionation according to the SI mechanism provides its concentration in implicit forms even at limited Au concentrations (<10 ppm). However, in the cases of pyrite–pyrrhotite and pyrite–hematite assemblages, native gold preferentially precipitates even at the Au solubility of 0.2–0.002 ppm owing to the greater probability of reaching this limit.

The preferential manifestation of the SI mechanism for mineral assemblages under the least reduced conditions is an important issue in technological mineralogy. The formation of high-grade bornite and chalcopyrite ores at many massive sulfide deposits [14] is consistent with the facies setting of enargite–digenite–pyrite–bornite–tennantite and bornite–pyrite–chalcopyrite assemblages. At the same time, precisely these ores are characterized by considerable losses of Au in the process of its gravitational recovery due to the existence of its implicit species [15].

REFERENCES

1. V. L. Tauson, A. G. Mironov, N. V. Smagunov, et al., Geol. Geofiz. **37** (3), 3 (1996).
2. V. L. Tauson, Eur. J. Mineral. **7**, 937 (1999).
3. V. L. Tauson, O. I. Bessarabova, R. G. Kravtsova, et al., Geol. Geofiz. **43** (1), 57 (2002).
4. V. L. Tauson, Geol. Geofiz. **40** (10), 1488 (1999).
5. A. M. Wilder and T. M. Seward, Geochim. Cosmochim. Acta **66**, 383 (2002).
6. G. Simon, H. Huang, J. E. Penner-Hahn, et al., Am. Mineral. **84**, 1071 (1999).
7. S. M. Zhmodik, A. P. Lisitsyn, V. A. Simonov, et al., Dokl. Earth Sci. **379A**, 649 (2001) [Dokl. Akad. Nauk **379**, 367 (2001)].
8. V. V. Fadeev and S. V. Koserenko, Geochem. Int. **37**, 1182 (1999) [Geokhimiya **37**, 1313 (1999)].
9. S. V. Koserenko, F. E. Wagner, J. Friedl, and V. V. Fadeev, Geochem. Int. **39** (Suppl. 2), S167 (2001).
10. Yu. V. Shvarov, Geochem. Int. **37**, 552 (1999) [Geokhimiya **37**, 646 (1999)].
11. N. N. Akinfiev and A. V. Zotov, Geochem. Int. **39**, 990 (1999) [Geokhimiya **39**, 1083 (2001)].
12. T. P. Dadze, G. A. Kashirtseva, R. Yu. Orlov, and V. I. Sorokin, in *Experimental and Theoretical Modeling of Mineral Formation* (Nauka, Moscow, 1988), pp. 387–393 [in Russian].
13. H. Hirsch, A. De Cugnac, M. Gadet, and J. Pouradier, C. R. Acad. Sci. **263**, 1328 (1966).
14. V. P. Moloshag, A. I. Grabezhev, I. V. Vikent'ev, and T. Ya. Gulyaeva, Litosfera, No. 2, 30 (2004).
15. I. V. Vikent'ev, V. P. Moloshag, A. I. Tsepin, et al., in *Proceedings of All-Russia Scientific Conference on Geology, Geochemistry, and Geophysics at the Eve of the 21st Century* (Svyaz-Print, Moscow, 2002), Vol. 2, pp. 237–238 [in Russian].